Heat Transfer and Fluid Flow Model for a High-speed Rotating Heat Pipe

Dominik Kern, Michael Groß

Institute for Applied Mechanics and Dynamics

26th March 2019

TECHNISCHE UNIVERSITÄT
CHEMNITZ

Potential Application

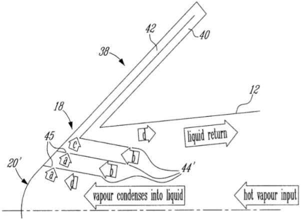

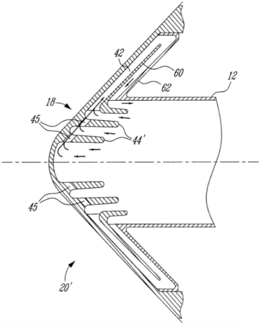

https://patents.google.com

Baseline Situation

We like to design a test bench for experiments..

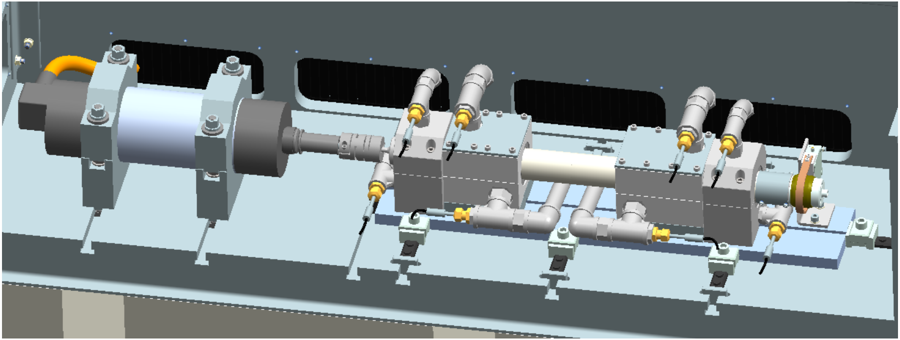

CAD model of a rotating heat pipe

Baseline Situation

..there is a promising model out there..

Available online at www.sciencedirect.com

SCIENCE DIRECT®

PERGAMON

International Journal of Heat and Mass Transfer 46 (2003) 4393–4401

International Journal of HEAT and MASS TRANSFER

www.elsevier.com/locate/ijhmt

Fluid flow and heat transfer model for high-speed rotating heat pipes

F. Song, D. Ewing, C.Y. Ching *

Department of Mechanical Engineering, McMaster University, Hamilton, Ont., Canada, L8S 4L7

Received 7 October 2002; received in revised form 17 May 2003

Abstract

A new complete model has been developed to predict the performance of high-speed rotating heat pipes with centrifugal accelerations up to 10 000 g. The flow and heat transfer in the condenser is modeled using a conventional modified Nusselt film condensation approach. The heat transfer in the evaporator has previously been modeled using a modified Nusselt film evaporation approach. It was found, however, that natural convection in the liquid film becomes more significant at higher accelerations and larger fluid loadings. A simplified evaporation model including the mixed convection is developed and coupled with the film condensation model. The predictions of the model are in reasonable agreement with existing experimental data. The effects of working fluid loading, rotational speed, and pipe geometry on the heat pipe performance are reported here.

Baseline Situation

..but its implementation is described very briefly.

momentum change at the interface due to phase transformation, vapor pressure drop, and vapor shear force at the interface. The hydrostatic pressure gradient term is often neglected in previous models but retained here so that the model can be applied to the cylindrical heat pipe. To evaluate the vapor effects, two non-dimensional ratios R_1 and R_2 are estimated based on a 1-D vapor flow.

$$R_1 = \frac{\tau_{v,\delta}}{\rho_l \omega^2 r(\sin\alpha - \cos\alpha \frac{d\delta}{dx})\delta} \quad \text{and} \quad R_2 = \frac{\Delta P_v / L}{\rho_l \omega^2 r(\sin\alpha - \cos\alpha \frac{d\delta}{dx})} \tag{11}$$

R_1 and R_2 represent the ratio of vapor shear stress at the interface and pressure gradient to the liquid driving force, respectively. The interfacial shear stress is calculated using the Blasius equation and the pressure gradient is estimated from the Bernoulli equation. For $\omega^2 r > 1000$ g, the typical values of R_1 and R_2 are less than 0.001 and hence the vapor effects are neglected by dropping the corresponding terms.

For any control volume in the liquid film (Fig. 1), the mass conservation can be written as

$$\dot{m}_{l,in} = \dot{m}_{l,out} + d\dot{m}_l \tag{12}$$

where the liquid mass flow rate at the cross section is given by

$$\dot{m}_l = \int_0^\delta 2\pi r \rho_l u_l \, dy \tag{13}$$

Heat transfer across the liquid film is simplified by assuming conduction only and neglecting the second-order convection term in Eq. (3).

$$k_l \frac{\partial^2 T}{\partial y^2} = 0 \tag{14}$$

The heat flux through the heat pipe inner wall and liquid film is balanced by the phase change at the liquid–vapor interface.

$$q_w = \frac{k_w (T_{w,i} - T_{w,o})}{R_i \ln(R_o/R_i)} \tag{15}$$

$$q_l = q_w = k_l (T_{sat} - T_{w,i})/\delta = h_{fg} d\dot{m}_l / (2\pi R_i dx) \tag{16}$$

The film condensation/evaporation model can be solved by coupling the liquid flow Eqs. (10)–(13) and heat transfer Eqs. (15) and (16). The liquid flow in the adiabatic section is similar to that in the condenser, but with no heat transfer.

2.3. Mixed convection evaporator model

At high accelerations ($\omega^2 r > 1000$ g) and low heat flux ($q < 200$ kW/m^2), nucleate boiling is suppressed and natural convection becomes dominant in the liquid film in the evaporator. Under these conditions, the liquid velocity profile depends on whether the flow is laminar or turbulent. In a boundary layer, the flow transitions from laminar to turbulent as the Ra number increases. The velocity profile for a turbulent boundary layer can be approximated by a 1/7th power law. The velocity profile predicted as a function of K ($K = Gr/Re^{5/2}$) for mixed convection over a horizontal plate [19] agrees well with this trend. In this instance, the velocity profile in the presence of mixed convection is approximated by a power law where the magnitude of the power depends on whether forced or natural convection dominates and if the flow is laminar or turbulent.

$$\frac{u_l}{U} = \left(\frac{y}{\delta}\right)^b \quad \text{where} \begin{cases} b = 1/3 & \text{when } 1 < Gr/Re^2 < 10,\ Ra < 10^9 \\ b = 1/4 & \text{when } Gr/Re^2 > 10,\ Ra < 10^9 \\ b = 1/7 & \text{when } Ra \geqslant 10^9 \end{cases} \tag{17}$$

The unknowns U and δ are determined from Eq. (12) and the integral momentum equation

$$\int_0^\delta \omega^2 r \left(\sin\alpha - \cos\alpha \frac{d\delta}{dx}\right) dy - \frac{\tau_w}{\rho_l} - \frac{\tau_{v,\delta}}{\rho_l} = \frac{d}{dx}\int_0^\delta u_l(u_l - U)\, dy + \frac{dU}{dx}\int_0^\delta u_l \, dy \tag{18}$$

where $\tau_{v,\delta} = C_{f,\delta}\rho_v u_v^2/2$ and $\tau_w = C_{f,w}\rho_l U^2/2$, in which $C_{f,\delta}$ is determined by the Blasius equation and $C_{f,w}$ using the results of Afzal and Hussain [20] for mixed convection over a horizontal plate

$$C_{f,w} = \begin{cases} 0.5 & (0 < K \leqslant 1) \\ 0.5K^{3/5} & (K > 1) \end{cases} \tag{19}$$

The mixed convection heat transfer in the liquid film is modeled by the correlation for mixed convection in a forced horizontal boundary layer with a transverse buoyancy force [21]

$$q_l = h_m (T_{w,i} - T_{sat}) = (Nu_m k_l / \delta)\Delta T \tag{20}$$

$$Nu_m^{7/2} = Nu_f^{7/2} + Nu_n^{7/2} \tag{21}$$

The forced convection is approximated using the modified Nusselt film evaporation model. In the case of low Reynolds number liquid flow, $Nu_f = 1$. Several empirical correlations have been recommended for natural convection under acceleration [11], in which the heat transfer rate is proportional to $(\omega^2 r)^a$ where $0.25 < a < 0.375$. The correlation by Korner reported by Marto [11] was adopted here for the natural convection induced by acceleration.

$$Nu_n = 0.133 Ra^{0.375} \tag{22}$$

2.4. Calculation scheme

The heat pipe is discretized into finite control volumes along its axial length. The film condensation model

(Eqs. (10)–(16)) and mixed evaporation model (Eqs. (17)–(22)), with the appropriate boundary conditions (Eqs. (5)–(8)), are solved iteratively for each control volume to ensure conservation of mass and energy. In the presence of excess fluid loading, the liquid film thickness at the evaporator end cap is initially assumed and the film thickness profile along the heat pipe is solved for numerically. The fluid loading is calculated and the evaporator end cap film thickness is changed till the loading approaches the given fluid loading. The grid is subsequently refined till results independent of the grid size are obtained.

2.5. Model validation

The current model for high-speed rotating heat pipes was verified by simulating the test cases examined experimentally by Ponnappan et al. [12]. It should be noted that the heat pipe tested by Ponnappan et al. [12] was charged with about 15 times the ideal fluid loading, where ideal fluid loading (100%) is defined as the fluid mass in the heat pipe such that the film thickness at the evaporator end cap is zero for a given rotational speed. The current model results for the heat transfer rate with the temperature difference across the liquid film in the condenser ΔT_c are in good agreement with the experimental data for rotational speeds in the range 10 000 to 30 000 rpm (Fig. 2). The Nusselt condensation model [8] significantly over predicts the experimental data (Fig. 2), since the model can not take into account the redistribution of the excess fluid throughout the pipe due to the high fluid loading. As the fluid loading increases, the liquid film thickness in the condenser becomes thicker with a consequent decrease of the conduction heat transfer across the film. Both previous models and the current model predict an increase of heat transfer with the rotational speed, which is opposite to that of the experimental data, the reasons for which are not known at this point.

In the current model, the liquid velocity profile is assumed based on physical arguments. A sensitivity analysis of the assumed velocity profile was performed to examine its influence on the accuracy of the model results. The heat transfer rates for different values of the exponent b (in Eq. (17)) were evaluated at 10 000 rpm and were found to be nearly identical, with a maximum error of 2% at ideal fluid loading. The choice of b affects the liquid film thickness distribution along the evaporator. The natural convection along the evaporator length, however, is enhanced with an increase in liquid film thickness resulting in almost a constant heat transfer in the evaporator for different values of b. For the case of very low fluid loadings, the contribution from natural convection is negligible and in this case the heat transfer is affected slightly by the choice of b. It can be concluded that the choice of b in the liquid velocity

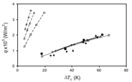

Fig. 2. Comparison between model predictions and experimental results [12]. ——, current model and – – –, Nusselt model at □, 10 000 rpm; △, 20 000 rpm; ○, 30 000 rpm with experimental data at the same speed represented by solid symbols.

profile has a negligible effect on the prediction of overall heat pipe performance, particularly for overcharged fluid loadings.

3. Results and discussion

The effects of fluid loading, rotational speed and taper geometry on the heat pipe performance were investigated using the present model. A constant wall temperature of 100 and 60 °C on the outside of the evaporator and condenser were used for the simulations. For consistency, the rotating heat pipe studied here has the same nominal dimensions (Table 1) as that tested by Ponnappan et al. [12].

3.1. Effect of fluid loading

The effect of fluid loading on the flow and heat transfer characteristics within the liquid film was initially investigated at 10 000 rpm using a 1° condenser taper. The ideal fluid loading (100%) is about 0.007 kg in this instance, which is defined as the fluid loading that gives a zero film thickness at the evaporator end cap. It is determined by solving for the liquid film thickness profile as well as the vapor flow through the heat pipe. The ideal fluid loading is significantly affected by the

Table 1
Nominal dimensions of rotating heat pipe

Length of evaporator/adiabatic/condenser	0.076/0.057/0.089 m
OD-pipe wall (stainless steel)	0.0254 m
ID-evaporator	0.0191 m
ID-condenser	0.016/0.0191 m
Adiabatic section taper angle	0°
Working fluid	Water

Model Description

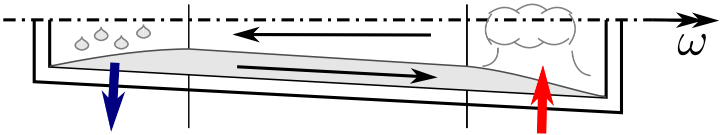

- axially rotating heat pipe in steady state
- heat transfer in condenser and evaporator only in radial direction, adiabatic section perfectly insulated
- high-speed rotating ($\omega^2 r \gg g$), gravity is neglected
- rotational symmetry
- thin liquid film, curvature effects negligible (cartesian instead of polar coordinates)
- one dimensional vapor flow

Liquid Flow Model for Condenser and Adabatic Section

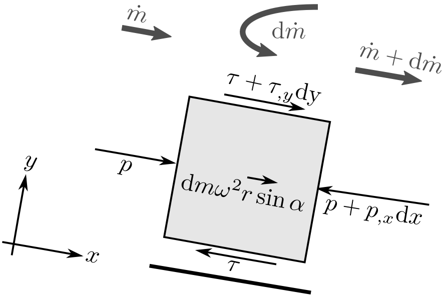

$$
\begin{aligned}
0 &\approx \rho_l \omega^2 r \sin\alpha - \frac{\partial p}{\partial x} + \frac{\partial \tau}{\partial y} \\
\tau(x, y=\delta) &= \frac{\mathrm{d}\dot{m}}{\mathrm{d}x}\Big(u_v \cos\alpha + u(x,\delta)\Big) \\
0 &= u(x, y=0)
\end{aligned}
$$

differential momentum bilance of liquid flow in x-direction (steady state)

Liquid Flow Model for Condenser and Adabatic Section

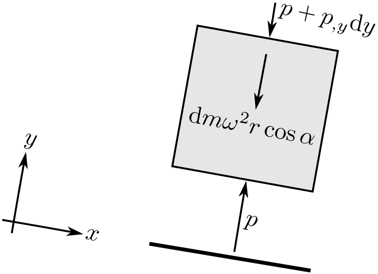

$$
\begin{aligned}
0 &\approx -\rho_l \omega^2 r \cos\alpha - \frac{\partial p}{\partial y} \\
p(x, y = \delta) &= p_{\mathrm{sat}}
\end{aligned}
$$

differential momentum bilance of liquid flow in y-direction (steady state)

Liquid Flow Model for Condenser and Adabatic Section

Assuming a thin liquid film ($r \approx R_i$), the y-direction of momentum bilance leads to

$$p(x,y) = p_{\mathrm{sat}} + \rho_l \big(\delta(x) - y\big)\omega^2 R_i .$$

Insertion of this pressure field $p(x,y)$ in the x-direction of momentum bilance and assuming a Newtonian Fluid $\tau = \mu_l \frac{\partial u}{\partial y}$ leads to

$$u(x,y) = \frac{\rho_l}{\mu_l}\omega^2 R_i \left(\sin\alpha - \frac{\mathrm{d}\delta}{\mathrm{d}x}\cos\alpha\right)\left(y\delta - \frac{1}{2}y^2\right) - \frac{y}{\mu_l}\frac{\mathrm{d}\dot{m}}{\mathrm{d}x}\Big(u_v\cos\alpha + u(u,\delta)\Big),$$

where vapor pressure drop and vapor shear stress have been neglected.

Heat Transfer Model for Condenser and Adabatic Section

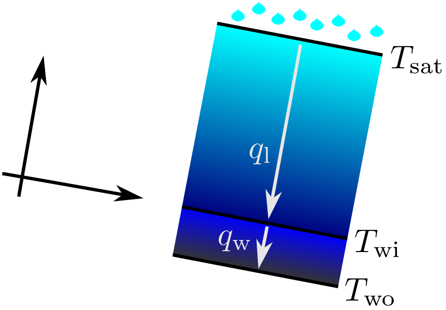

$$q_c = \frac{h_{\text{fg}}}{2\pi R_i} \frac{\mathrm{d}\dot{m}}{\mathrm{d}x}$$

$$q_l = \frac{k_l (T_{\text{sat}} - T_{\text{wi}})}{\delta}$$

$$q_w = \frac{k_w (T_{\text{wi}} - T_{\text{wo}})}{R_i \ln(R_o/R_i)}$$

radial heat transfer in steady state assuming film condensation

Notes:

- in steady state $q_c = q_l = q_w$
- in adiabatic section there is no heat flux: $q_l = q_w = 0 \rightsquigarrow \dfrac{\mathrm{d}\dot{m}}{\mathrm{d}x} = 0.$

Liquid Flow Model for Evaporator

Different than condenser, as experiments revealed occurence of natural convection at high accelerations in the evaporator.

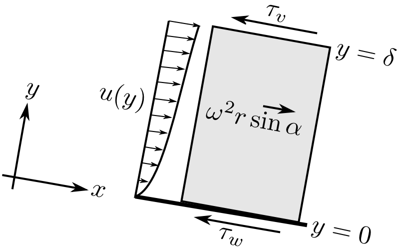

$$
\begin{aligned}
u(x,y) &= \left(\frac{y}{\delta(x)}\right)^b U(x) \\
b &= f(Gr, Re, Ra)
\end{aligned}
$$

$$
\int_0^\delta \rho_l \frac{\mathrm{d}u}{\mathrm{d}t}\,\mathrm{d}y = \int_0^\delta f(x,y)\,\mathrm{d}y - \tau_v - \tau_w
$$

integral momentum equation for transition from laminar to turbulent flow

Liquid Flow Model for Evaporator

Using Blasius Equation for the vapour shear stress [Daniels & Al-Jumaily 1975]

$$\tau_v = \frac{1}{2} C_v \rho_v u_v^2 \quad \text{with} \quad C_v = \begin{cases} \frac{16}{Re_v} & (Re_v \leq 2000) \\ \frac{0.0791}{Re_v^{0.25}} & (Re_v > 2000) \end{cases} \quad \text{and} \quad Re_v = \frac{u_v A}{\nu_v}$$

and a model for mixed convection over a horizonal plate [Afzal & Hussain 1984]

$$\tau_w = \frac{1}{2} C_w \rho_l U^2 \quad \text{with} \quad C_w = \begin{cases} 0.5 & (0 < K \leq 1) \\ 0.5 K^{3/5} & (1 < K) \end{cases} \quad \text{and} \quad K = Gr/Re^{5/2}$$

leads to an equation for the liquid velocity at the interface $U = u(x, y = \delta)$

$$\frac{\mathrm{d}}{\mathrm{d}x} \int_0^\delta u(u - U)\mathrm{d}y + \frac{\mathrm{dU}}{\mathrm{d}x} \int_0^\delta u\mathrm{d}y = \int_0^\delta \omega^2 r \left(\sin\alpha - \frac{\mathrm{d}\delta}{\mathrm{d}x} \cos\alpha \right) \mathrm{d}y - \frac{C_v}{2} \frac{\rho_v}{\rho_l} u_v^2 - \frac{C_w}{2} U^2.$$

Heat Transfer Model for Evaporator

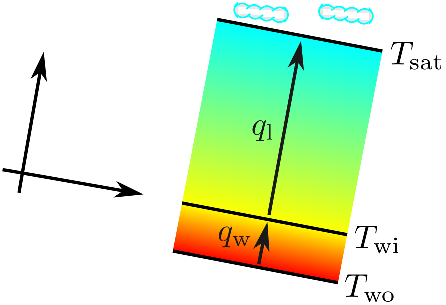

$$q_c = -\frac{h_{\mathrm{fg}}}{2\pi R_i}\frac{\mathrm{d}\dot{m}}{\mathrm{d}x}$$

$$q_l = \frac{Nu_m k_l (T_{\mathrm{wi}} - T_{\mathrm{sat}})}{\delta}$$

$$q_w = \frac{k_w (T_{\mathrm{wo}} - T_{\mathrm{wi}})}{R_i \ln(R_o/R_i)}$$

radial heat transfer in steady state assuming mixed convection

Nusselt Number for mixed convection [Marto 1984, Churchill 1990]

$$Nu_m{}^{7/2} = Nu_f^{7/2} + Nu_n^{7/2} \quad \text{with} \quad Nu_f = 1 \quad \text{and} \quad Nu_n = 0.133 Ra^{0.375}.$$

Discretization

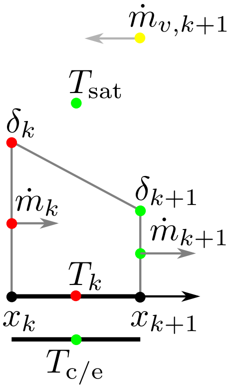

kth finite volume

known/prescribed:

vapour temperature T_{sat} (set in outer iteration)
right film height δ_{k+1} (starting from given B.C.)
mass flow out $\dot{m}_{k+1}$ (starting from given B.C.)
outer wall temperature $T_{\text{c/e}}$ (condenser/evaporator)

dependent:

vapour mass flow in steady state $\dot{m}_v = \dot{m}$
difference in mass flow $\Delta\dot{m}_k = \dot{m}_{k+1} - \dot{m}_k$

unknown:

left film height δ_k
mass flow in $\dot{m}_k$
inner wall temperature T_k

Discretization

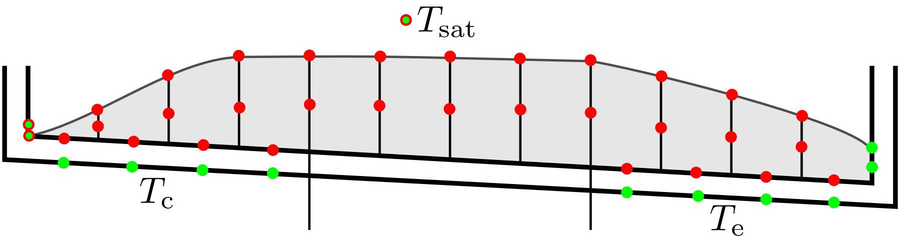

complete heat pipe filling: prescribed and unknown quantities

- film height δ_{N+1} at evaporator end corresponds to filling ratio and is prescribed
- mass flow $\dot{m}_{N+1}$ at evaporator end is zero (no flow through wall)
- vapour temperature T_{sat} is found in outer iteration (and fixed for inner iterations)
- outer search minimizes mass flow $\dot{m}_1$ at condenser end (no flow through wall)

Inner Iterations

Equations for liquid flow and heat transfer are approximated by **finite differences** for derivatives and **mid-point rule** for integrals.

Both models relate film height with difference in mass flow

$$\begin{aligned} \Delta\dot{m}_k^{\mathrm{lf}} &= f^{\mathrm{lf}}(\delta_k, \delta_{k+1}, \dot{m}_{k+1}), \\ \Delta\dot{m}_k^{\mathrm{ht}} &= f^{\mathrm{ht}}(\delta_k, \delta_{k+1}, \dot{m}_{k+1}). \end{aligned}$$

For each finite volume, from evaporator to condenser (adiabatic section simplifies to $\Delta\dot{m}_k^{\mathrm{ht}} = 0$), the left film height δ_k is iterated by **regula falsi** until both models match

$$\Delta\dot{m}_k^{\mathrm{lf}} \approx \Delta\dot{m}_k^{\mathrm{ht}}.$$

If there is no convergence, then the iterations are **restarted** with a new initial guess δ_k^0.

Outer Search

Inner iterations: $T_{\text{sat}} \rightsquigarrow \dot{m}_1$ (mass flow through wall)

Outer search: find T_{sat}, such that $\dot{m}_1 = 0$ (impermeable wall)

Problem: some finite volumes do not converge $\rightsquigarrow$ iterative methods lead astray.

Solution: use grid points for T_{sat} and interpolate only converged results.

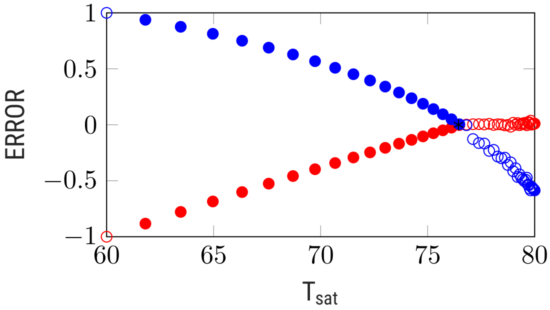

mass flow through wall ($\dot{m}_1$) and heat bilance ($Q_{\text{in}} - Q_{\text{out}}$) vs. vapour temperature

Results

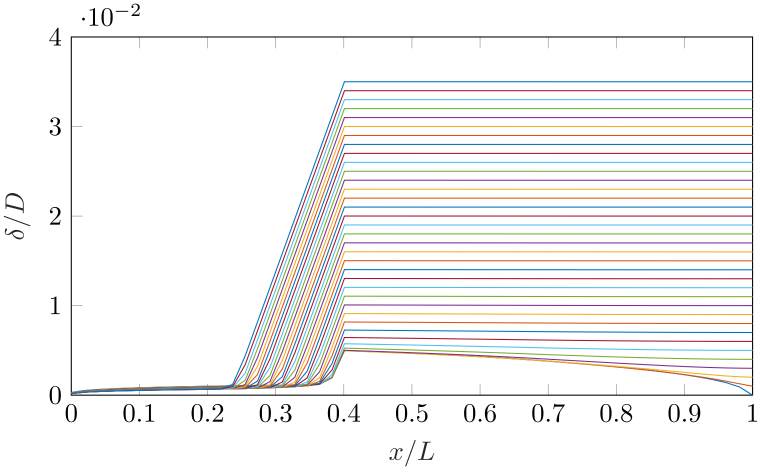

liquid film thickness vs. axial position

Results

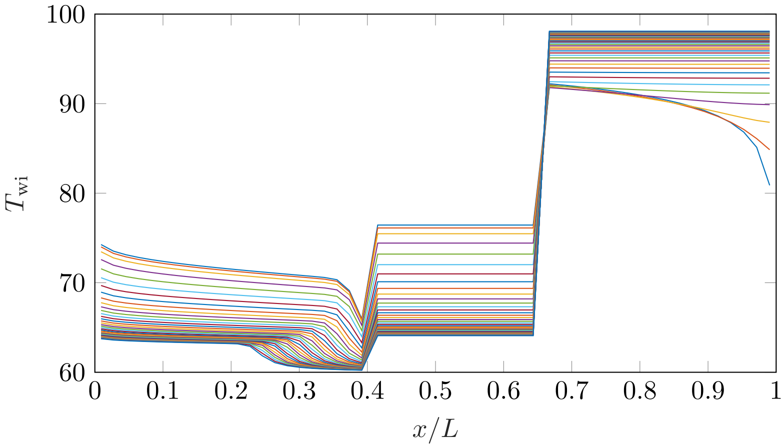

inner wall temperature vs. axial position

Results

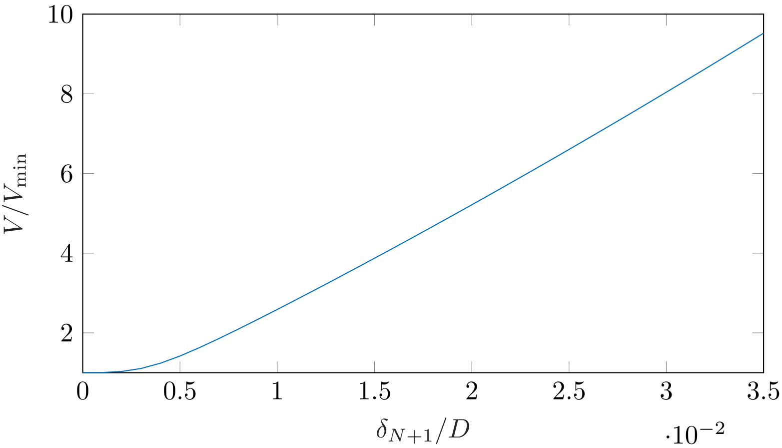

liquid volume vs. film thickness at evaporator end

Results

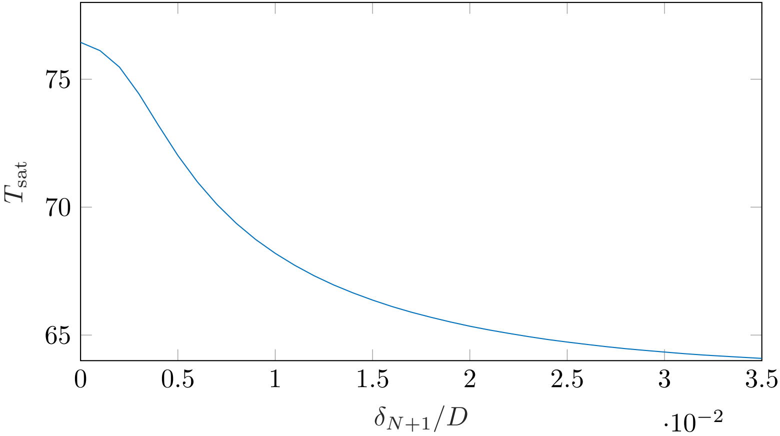

vapour temperature vs. film thickness at evaporator end

Results

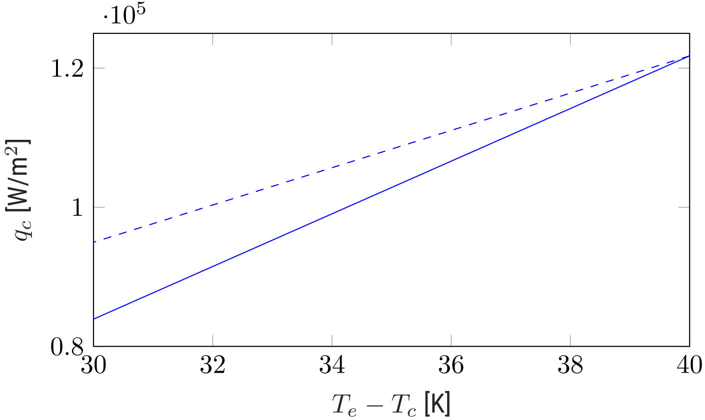

heat flux vs. temperature difference
(solid line – reference fluid loading, dashed line – ideal fluid loading)

Results

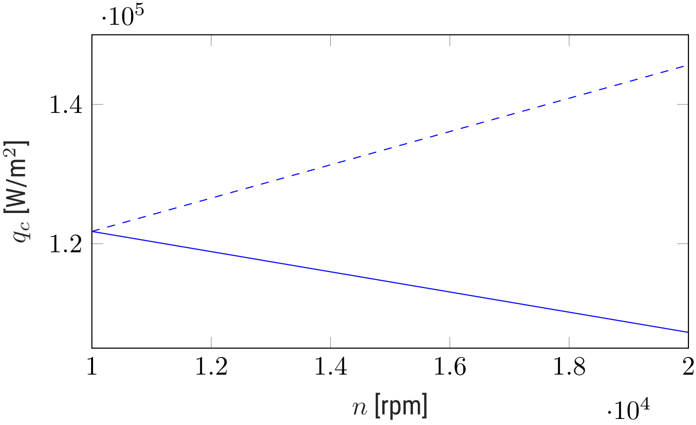

heat flux vs. rotational speed
(solid line – reference fluid loading, dashed line – ideal fluid loading)

The results are in reasonable agreement with experimental data [Song et. al. 2003], where the fluid flow and heat transfer inside a rotating heat pipe

- has been modeled by reduced Navier-Stokes Equations and Handbook formula for heat transfer and convection,
- and discretized by finite volumes (one-dimensional).

The reproduction of the results caused some efforts, so we strongly recommend:

AIMS Mathematics

http://www.aimspress.com/journal/Math

AIMS Mathematics, 1(3): 261-281
DOI:10.3934/Math.2016.3.261
Received: 27 June 2016
Accepted: 1 September 2016
Published: 28 September 2016

Review

Best practices for replicability, reproducibility and reusability of computer-based experiments exemplified by model reduction software

Jörg Fehr[1], Jan Heiland[2], Christian Himpe[3,*], and Jens Saak[2]

Example [Song et. al. 2003]

k	$0.598\,\frac{\mathrm{W}}{\mathrm{m\cdot K}}$	thermal conductivity
ϱ	$998\,\frac{\mathrm{kg}}{\mathrm{m}^3}$	density
μ	$1.002\cdot 10^{-3}\,\mathrm{Pa\cdot s}$	dynamic viscosity
β	$\frac{1}{3}\cdot 207\cdot 10^{-6}\,\mathrm{K}^{-1}$	thermal expansion (length)
c_p	$4186\,\frac{\mathrm{J}}{\mathrm{kg\cdot K}}$	heat capacity
h_{fg}	$2.257\cdot 10^{6}\,\frac{\mathrm{J}}{\mathrm{kg}}$	latent heat

liquid parameters (water)

Example [Song et. al. 2003]

ϱ	$0.768\,\frac{\mathrm{kg}}{\mathrm{m}^3}$	density
μ	$12.4 \cdot 10^{-6}\,\mathrm{Pa}\cdot\mathrm{s}$	dynamic viscosity

vapour parameters (water)

k	$45\,\frac{\mathrm{W}}{\mathrm{m}\cdot\mathrm{K}}$	thermal conductivity

pipe parameters (steel)

Example [Song et. al. 2003]

δ_{N+1}/D_i	$0.000 \ \ldots \ 0.035$	relative film heigth at e. end
T_c, T_e	$60°\mathrm{C}, 100°\mathrm{C}$	outer wall temperature at c./e.
ω	$\frac{2\pi}{60} \cdot 10 \cdot 10^3\,\mathrm{RAD} \cdot \mathrm{s}^{-1}$	angular velocity
L_c, L_a, L_e	$89\,\mathrm{mm}, 57\,\mathrm{mm}, 76\,\mathrm{mm}$	c./a./e. length
R_o	$12.7\,\mathrm{mm}$	constant outer radius
$R_{i,c}, R_{i,a}, R_{i,e}$	$8 - 9.55\,\mathrm{mm}, 9.55\,\mathrm{mm}, 9.55\,\mathrm{mm}$	inner radius c./a./e.
$\alpha_c, \alpha_a, \alpha_e$	$2°, 0°, 0°$	taper angle c./a./e.

geometry and operational parameters

Example [Song et. al. 2003]

N_c, N_a, N_e	$23, 10, 19$	finite volumes per condenser/adiabatic/evaporator
$\varepsilon_{\dot{m},i}$	10^{-6}	relative tolerance for FV iterations
$\varepsilon_{\dot{m},C}$	10^{-2}	relative tolerance for outer search
$N_{\mathrm{max,iterations}}$	100	maximum number of FV iterations
$N_{\mathrm{max,restarts}}$	38	maximum number of FV restarts
$N_{\mathrm{max,outer}}$	50	grid points for outer loop
M_{mean}	50	iterations after which an accelerated step is done

discretization parameters